FASEB BioAdvances WILEY

Biophysical characterization of lynx-nicotinic receptor interactions using atomic force microscopy

Avani V. Pisapati[1] | **Wenpeng Cao**[1] | **Kristin R. Anderson**[2] | **Griffin Jones**[2] | **Katie Hoffman Holick**[2] | **Paul Whiteaker**[5] | **Wonpil Im**[1,2,4] | **X. Frank Zhang**[1,3] | **Julie M. Miwa**[2]

[1]Department of Bioengineering, Lehigh University, Bethlehem, Pennsylvania, USA

[2]Department of Biological Sciences, Lehigh University, Bethlehem, Pennsylvania, USA

[3]Department of Mechanical Engineering and Mechanics, Lehigh University, Bethlehem, Pennsylvania, USA

[4]Department of Chemistry, Lehigh University, Bethlehem, Pennsylvania, USA

[5]Division of Neurobiology, Barrow Neurological Institute, St. Joseph's Hospital and Medical Center, Lehigh University, Phoenix, Arizona, USA

Correspondence

Julie M. Miwa, Department of Biological Sciences, Lehigh University, 111 Research Drive, Bethlehem, PA 18015, USA.
Email: jmm312@lehigh.edu

X. Frank Zhang, Department of Bioengineering, Lehigh University, 111 Research Drive, Bethlehem, PA 18015, USA.
Email. xiz310@lehigh.edu

Abstract

Nicotinic acetylcholine receptors (nAChRs) are broadly expressed in the central and peripheral nervous systems, playing essential roles in cholinergic neurotransmission. The lynx family proteins, a subset of the Ly6/uPAR superfamily expressed in multiple brain regions, have been shown to bind to nAChRs and modulate their function via allosteric regulation. The binding interactions between lynx and nAChRs, however, have not been systematically quantified and compared. In this work, we characterized the interactions between lynx1 or lynx2 and α3β4- or α7-nAChRs using single-molecule atomic force microscopy (AFM). The AFM technique allows the quantification of the off-rate of lynx-nAChR binding and of the energetic barrier width between the bound state and transition state, providing a biophysical means to compare the selectivity of lynx proteins for nAChR subtypes. Results indicate that lynx1 has a marginal preference for α7- over α3β4-nAChRs. Strikingly, lynx2 exhibits a two order of magnitude stronger affinity for α3β4- compared to α7-nAChRs. Together, the AFM assay serves as a valuable tool for the biophysical characterization of lynx-nAChR binding affinities. Revealing the differential affinities of lynx proteins for nAChR subtypes will help elucidate how lynx regulates nAChR-dependent functions in the brain, including nicotine addiction and other critical pathways.

KEYWORDS

atomic force microscopy, lynx1 protein, lynx2 protein, nicotine addiction, nicotinic acetylcholine receptors, snake venom toxins

1 | INTRODUCTION

Nicotinic acetylcholine receptors (nAChRs) are broadly expressed in the brain and respond to nicotine, the major psychoactive ingredient in tobacco. Tobacco use results in approximately 480,000 deaths each year and costs more than $300 billion dollars annually in the USA alone. Understanding nAChR activity and its modulation in nicotine addiction, therefore, has significant public health implications.[1,2] At the same time, evidence supports that nicotine may provide positive benefits in some disease states, including neuroprotection from Parkinson's disease and counterbalancing the dysfunction of dopaminergic, glutamatergic, and GABAergic pathways in schizophrenia.[3,4] Nicotine's diverse contributions to disease thus require demarcating its distinct effects on different brain regions, neuronal circuits, nAChR subtypes, and regulatory mechanisms.

nAChRs are pentamers composed of a combination of subunits α1-α10, β1-β4, γ, δ, and ε. Each nAChR subtype's composition determines its unique pharmacological and biophysical characteristics and can be associated with a specific pathophysiological process and brain region.[5–7] For example, a two base pair deletion in the duplicate α7 subunit gene has been associated with increased schizophrenia risk.[8,9] As a further example, mutations in the α4 and β2 nAChR subunits, which are highly expressed in the thalamus and cortex, have been associated with increased risk for autosomal dominant nocturnal frontal epilepsy (ADNFE), where changes in the function of α4β2-nAChR subunits may perturb thalamocortical networks and trigger seizures.[10–12] Human GWAS mapping also supports that single nucleotide polymorphisms that confer more significant nicotine addictive propensity can be found on the α5, α3, and β4 gene cluster on chromosome 15.[13] nAChRs containing these subunits are found in greater numbers in the ventral medial habenula (MHbV) and interpeduncular nucleus (IPN), with α3 and β4 subunits localized in the MHbV and α5 in the IPN, as shown in multiple animal studies.[14,15] These findings indicate that the MHbV-IPN pathway may be implicated in nicotine addiction, and further understanding of the nAChR subtypes expressed in it could be critical for elucidating addiction mechanisms.

It has previously been discovered that nAChRs are allosterically modulated by small three-fingered proteins known as prototoxins, expressed endogenously on the surface of neurons in the brain.[16] Prototoxin genes are named after their shared evolutionary origins with the snake alpha-neurotoxin gene precursors, whose protein products are known to bind to nicotinic receptors and are part of the ly-6/neurotoxin superfamily.[16,17] By binding to nAChRs, these proteins can fine-tune the widespread, excitatory cholinergic system, a system that provides control over multiple neural circuits.[18] This has been shown to have a wide variety of physiological effects, affecting multiple mechanisms of nAChR function, including receptor assembly, expression, binding specificity, as well as receptor desensitization, and agonist affinity.[18,19] Two members of this group include lynx1 and lynx2, which contain the three-fingered receptor binding toxin motif of the Ly6/neurotoxin superfamily and are glycosylphosphatidylinositol (GPI)-anchored membrane proteins, differentially expressed in different regions and neurons throughout the brain.[18]

Lynx1 has been shown to regulate plasticity in the hippocampus,[20,21] alter plasticity in the adult visual and auditory cortices[20] and suppress associative learning and memory.[9] More specifically, it has been shown to associate with α4β2-nAChRs and to increase the rate of receptor desensitization to acetylcholine.[22] It also has an overall inhibitory effect on the nAChR function of α3, β4, and α5-containing nAChR subtypes by decreasing the number of $(\alpha3\beta4)_2\alpha5$- and $(\alpha3\beta4)_2\beta4$-nAChRs on the neuronal cell membrane and reducing the single-channel function of $(\alpha3\beta4)_2\alpha5$- and $(\alpha3\beta4)_2\alpha3$-nAChRs.[23] This supports the possibility that lynx1 modulates nAChRs containing the α5, α3, and β4 subunits implicated in the MHbV-IPN pathway relevant to addiction. Other subtypes, such as α7-nAChRs, have also been shown to be affected by lynx1.[9]

Lynx2 is a family member to lynx1, with expression in anxiety-specific brain regions distinct from that of lynx1.[24,25] On a biophysical level, the two proteins have been shown to display similar functional characteristics, such as α4β2-nAChR binding in co-IP studies[26,27] and acceleration of desensitization kinetics.[22,24] Additionally, lynx2 has been shown to have effects on nAChR assembly, including reduction of the receptor's cell surface expression,[27] and has been shown to be expressed in the amygdala and prefrontal cortex.[24,25] Plus, the removal of its gene in mice results in anxiety-like behaviors.[24] However, a full understanding of these proteins' effects and specificity on the many nAChR subtypes are still nascent. The diversity of characterization methods used in previous studies require the measurement of a single quantity that compares the binding affinities of lynx proteins for relevant nAChR subtypes for specific behavioral states or phenotypes.

Atomic force microscopy (AFM) is an ultrasensitive force spectroscopy technique that can be used to measure bond ruptures between two molecules in the piconewton (pN) range.[28] In this technique, a ligand can be functionalized to an AFM cantilever while a receptor is expressed on a whole cell. The deflection of the cantilever as it approaches and retracts from the whole cell can then be used to measure the force of the ligand-receptor interaction and, in turn, the dynamic strength of the complex and the free energy changes it undergoes during rupture.[29] In this paper, we used AFM[30,31] to quantify and compare the binding affinity between α3β4- or α7-nAChRs expressed

on cells and lynx1 or lynx2 proteins functionalized to an AFM tip. This method allows us to precisely characterize the off-rate of lynx-nAChR binding and the energetic barrier width between the bound state and transition state, providing a means to compare the selectivity of lynx1 and lynx2 for α3β4- and α7-nAChRs. These quantitative findings ultimately indicate that lynx1 has a slight preference for α7- compared to α3β4-nAChRs, while lynx2 exhibits a stronger affinity for α3β4-nAChRs. Additionally, while α7-nAChRs have a similar affinity for lynx1 and lynx2, α3β4-nAChRs have a higher affinity for lynx2 than lynx1. Understanding the differential affinities of lynx proteins for various nAChR subtypes more precisely is a valuable starting point to better understand the nature of their interactions and selectivity. In turn, this will help to illuminate the lynx-nAChR complexes that have important roles in normal and disease physiology, as outlined previously.

2 | MATERIALS AND METHODS

2.1 | Protein expression

Both recombinant lynx1 and lynx2 proteins were synthesized from *Escherichia coli* and purified. Wild-type (WT) lynx genes were inserted into pET-14b-6xHis plasmids (GenScript BioTech) transformed into One-Shot BL21 (DE3) Chemically Competent *E. coli* (Invitrogen, ThermoFisher Scientific) and induced with isopropyl β-D-1-thiogalactopyranoside (IPTG). The His-tagged lynx proteins were eluted from nickel columns by Ni-NTA elution buffer. All chemicals used to make the buffers for the nickel column protein purification came from Sigma-Aldrich Corporation. Samples were then dialyzed at 4℃ overnight in 8 M urea and subsequently with progressive twofold dilutions in PBS. The dialyzed protein and the purified elutions of each sample were run on SDS-PAGE gel (Bio-Rad Laboratory) in order to confirm protein purity and yield. Water-soluble lynx1 has been shown to maintain the functional effects of the native GPI-anchored protein,[16,26,32] demonstrating the correct folding of soluble lynx1 proteins.

2.2 | Cell lines

The stably transfected SH-EP1-hα7-nAChR cell line was previously engineered and characterized as described in Zhao et al.[33] The engineering of the new stably transfected SH-EP1-hα3β4-nAChR cell line was very similar to that previously described for a stably transfected SH-EP1-hα6/3β2β3-nAChR cell line.[28] In summary, WT SH-EP1 cells were transfected with nAChR subunit clones using Effectene (Qiagen). Human nAChR α3 and β4 subunit

genes optimized for vertebrate expression were used. These were synthesized and sequenced for confirmation by Invitrogen GeneArt, ThermoFisher Scientific. Sequences corresponded to human consensus sequences. Double-transfectants were created by transfection of the α3 subunit in the pcDNA3.1zeo vector and the β4 subunit in the pcDNA3.1hygro vector (Invitrogen, ThermoFisher Scientific). Positive selection was imposed with hygromycin B (0.4 mg/ml, 0.13 mg/ml biologically active hygromycin, EMD Millipore) and zeocin (0.25 mg/ml, Invitrogen, ThermoFisher Scientific). The selected, surviving monoclones were picked and then screened for radioligand binding using [^{3}H]epibatidine binding (500 pM, 52 Ci/mmol, Perkin-Elmer). Non-specific binding was defined in the presence of 1 mM (-)-nicotine and subtracted from total binding to define nAChR-specific binding. The monoclones with the highest levels of specific [^{3}H]epibatidine binding were chosen to be assessed for nAChR function using ^{86}Rb$^+$ efflux assays as previously described.[34] Total ^{86}Rb$^+$ efflux was measured in the presence of 100 μM carbamylcholine, and specific efflux was determined as the difference between total and nonspecific efflux (that was measured in the presence of the noncompetitive antagonist mecamylamine; 100 μM, sufficient to completely block nAChR activation). The clone, which consistently exhibited the highest specific ^{86}Rb$^+$ efflux, was selected. The resulting SH-EP1-hα3β4-nAChR monoclone was then maintained under positive selection using the same concentration of hygromycin and zeocin as just described. Low passage number cultures were used (1–40 from frozen stocks), ensuring the stable expression of the phenotype. Both cell lines were passaged once weekly by splitting cultures 1/20−1/40, just before they reached confluency. In this way, cells could be maintained in a proliferative growth phase.

2.3 | Single-molecule force spectroscopy

Single-molecule experiments testing lynx-nAChR interactions were conducted using a custom-built AFM optimized for studying protein–protein interactions.[35] A schematic of our homemade AFM system is shown in Figure 1A. Lynx proteins were attached to an AFM cantilever by covalently crosslinking the two using a heterobifunctional PEG linker.[36] The AFM cantilevers (MLCT-Bio-DC: Bruker Nano) were first silanized with (3-aminopropyl)triethoxysilane (APTES) using a gas phase coating method.[37] An acetal-PEG27-NHS linker was then attached to the silanized cantilevers in chloroform via its NHS group and then rinsed and dried under nitrogen gas. Next, the acetal group of the PEG linker was converted to an aldehyde group using a 1% citric acid solution, and 1 μM of lynx protein was then added to the solution, which coupled to the activated PEG
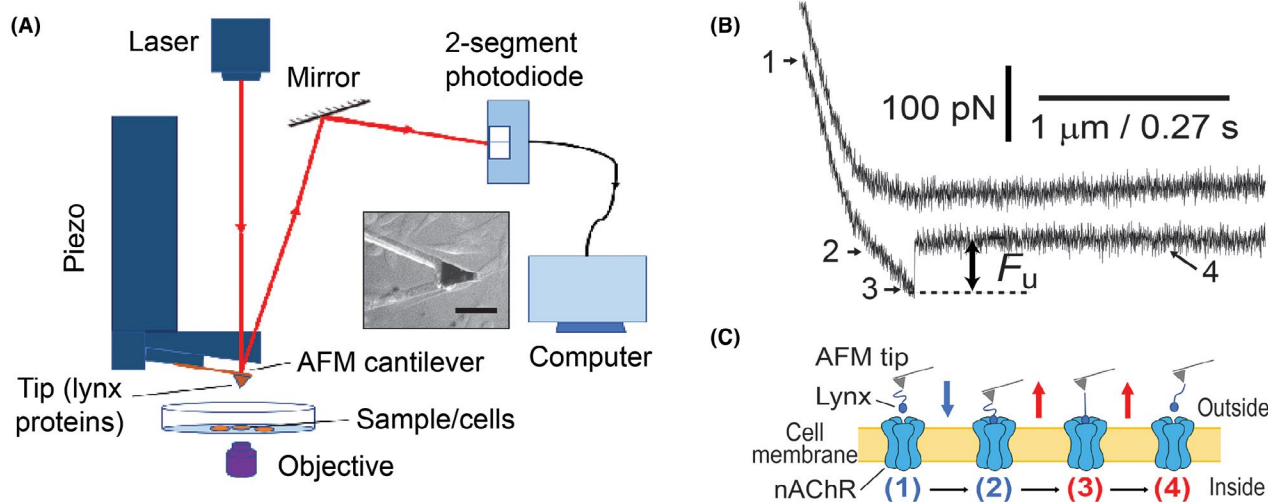
FIGURE 1 The unbinding force detection of lynx-nicotinic acetylcholine receptor (nAChR) interactions. (A) Schematic of the custombuilt atomic force microscope (AFM). Inset: a micrograph showing an AFM microcantilever functionalized with lynx2 above SH-EP1 cells expressing the α7-nAChR. The scale bar is 50 mm. (B) Representative pulling traces. The upper trace had no interaction, and the lower trace shows the rupture force of a single lynx2−α7-nAChR complex. F_u is the unbinding force. k_s is the system spring constant and was derived from the slope of the force-displacement trace. The cantilever retraction rate of the measurements was 3.7 μm/s. The four stages of stretching and rupturing a single ligand-receptor complex are labeled on the red trace. More representative pulling traces are shown in Figure S1. (C) The four stages of force measurement: 1. The functionalized cantilever moves downward to allow contact with a cell membrane. 2. A small constant force (250 pN) is applied onto the membrane, providing the time and space for a ligand-receptor interaction to occur. 3. The AFM tip retracts from the cell membrane. If the protein is bound to a receptor, an adhesive force resists separation between the tip and cell membrane. 4. The ligand-receptor interaction ruptures, and the cantilever unbinds

linker. Different SH-EP1 cell lines (untransfected WT control cells (WT), α3β4 or α7) were grown on 35 mm cell culture dishes. Individual cells in the dish were aligned under the lynx-coated AFM tip (Figure 1A). The tip was then directed to approach toward and retract from the cell surface, and the computer recorded the rupture force between the protein and receptor during the process (Figure 1B,C). To calibrate the cantilever (320 μm long by 22 μm wide triangle), the spring constant at the tip was characterized via thermally induced fluctuations.[38] The spring constants (10.2 ± 2.1 pN/nm, mean ± SD) of the calibrated cantilevers agreed with the values specified by the manufacturer (10 pN/nm). Different tip retraction speeds were applied to obtain the rupture force during different loading rates (0.94, 1.88, 3.76, and 7.52 μm/s). A similar AFM assay has been utilized by us[39–42] and others[43–45] to study a variety of protein–protein interactions on cell surfaces.[46] Loading rates of the rupture forces were determined from each unbinding force curve by conducting a linear fit to the force-time curve shortly (the last 50 data points) before rupture.

2.4 | Biophysical model analysis

The Bell–Evans model, a theory to determine energy landscape properties, describes an external force's influence on the bond dissociation rate.[47,48] According to this model,

a pulling force f distorts the intermolecular potential of a ligand-receptor complex, leading to lower activation energy and an increase in the dissociation rate $k(f)$ as follows:

$$k(f) = \frac{1}{t(f)} = k^0 \exp\left(\frac{f\gamma}{k_B T}\right),\tag{1}$$

where f is an external force in N, k^0 is the dissociation rate constant in the absence of a pulling force, γ is the width of the activation barrier, or the position along the reaction coordinate relative to the bound state, T is the absolute temperature and k_B is the Boltzmann's constant ($1.3806488 \times 10^{-23}$ m^2 kg s^{-2} K^{-1}). For a constant loading rate r_f, is the probability density for the unbinding of the complex as a function of the pulling force f is given by:

$$P(f) = k0 \exp\left(\frac{\gamma f}{kBT}\right) \exp\left\{\frac{k0kBT}{\gamma rf}\left[1 - \exp\left(\frac{f\gamma}{kBT}\right)\right]\right\}\tag{2}$$

with the most probable unbinding force $f*$ being:

$$f* = \frac{kBT}{\gamma}\ln\left(\frac{\gamma}{k0kBT}\right) + \frac{kBT}{\gamma}\ln(rf).\tag{3}$$

Hence, the Bell model predicts that the most probable unbinding force $f*$ is a linear function of the logarithm of the loading rate. Experimentally, $f*$ is determined from the mode of the unbinding force histograms. The Bell model

parameters k^0 and γ were determined by fitting Equation (3) to the plot of f^* versus $\ln(r_f)$.

2.5 | Statistical analysis

For each pulling speed, over 200 force curves were recorded. Curve fitting was performed using IGOR Pro or Origin software by minimizing the chi-squared statistics for the optimal fit. Unless otherwise stated, the data are reported as the mean and the standard error of the estimate. Statistical analyses of the linear regression were conducted using Analysis of Covariance (ANCOVA) by the Prism software (GraphPad Software), with a p-value less than 0.05 considered statistically significant.

3 | RESULTS

In order to quantify the differential affinities of lynx1 and lynx2 for $\alpha3\beta4$- and $\alpha7$-nAChRs, we used AFM to obtain the off-rate k^0 and the energetic barrier distance γ between the bound state and transition state of the prototoxin-receptor pair interaction. To obtain this data, both lynx1- and lynx2-coated AFM tips were lowered down to cells expressing $\alpha3\beta4$- and $\alpha7$-nAChRs and then retracted, where each retraction represented one scan (Figure 1B,C). We found that large rupture forces (typically greater than 40 pN) were observed during 30%–40% of the AFM scans. This value of 30%–40%, referred to as the adhesion frequency, was compared to the 10% adhesion frequency of small forces (<40 pN) observed between both lynx proteins and WT control cells that did not express any nAChRs. According to Poisson statistics, this indicated that both lynx1 and lynx2 specifically bound to the nAChRs and that each scan represented an interaction between a single lynx molecule and a single nAChR (>80% probability).[49] These results are shown in Figure 2.

The unbinding force F_u detection values, representing the unbinding force between each lynx-nAChR pair in pN, were obtained at varying loading rates or various retraction speeds of the AFM tip (pN/s) (Figure 1B). These loading rates were used to extract binding kinetics from the Bell–Evans model.[47,48] For each lynx-nAChR pair, the loading rate versus the most probable unbinding force at each loading rate obtained from force histograms (Figure S2) were plotted in Figure 3A. Figure 3A illustrates that the unbinding forces of lynx1-$\alpha3\beta4$, lynx1-$\alpha7$, and lynx2-$\alpha7$ fell in a similar range of 50–90 pN. Lynx2-$\alpha3\beta4$ unbinding forces, however, were stronger (87–122 pN) under the respective loading rates, indicating that the lynx2-$\alpha3\beta4$ interaction could be stronger than the other three interactions.

This data were then fitted to the Bell–Evans model (Equation 3), allowing us to obtain the off-rate k^0 and energetic barrier distance γ, as shown in Table 1. These data support that lynx1-$\alpha3\beta4$, lynx1-$\alpha7$, and lynx2-$\alpha7$ interactions had off-rates with the same order of magnitude (within fitting error and ~10^{-2} s^{-1}) and similar γ (0.4–0.5 nm). However, the lynx2-$\alpha3\beta4$ interaction was stronger, with a two orders of magnitude decrease in off-rate (although the value of γ remained similar to those of the other three interactions measured).

Since the energetic barrier distance and dissociation constants and energetic barrier distance were obtained from the Y-intercepts and slops of the linear regression fits, respectively (Equation 3), we conducted statistical analyses of the slopes and intercepts of the linear regression using Analysis of Covariance (ANCOVA), shown in Figure 3B,C. The ANCOVA results indicate the slopes of the four linear regression fits shown in Figure 3A are not significantly different ($p = 0.24$) (Figure 3B), confirming that the energetic barrier distances of the four tested lynx-receptor interactions are not significantly different. However, the analysis shows that the intercept of the linear fit for the lynx2-$\alpha3\beta4$ interaction is significantly larger than any of the other three interactions ($p < 0.001$) (Figure 3C), and that the intercepts among the other three interactions (i.e., lynx1-$\alpha3\beta4$, lynx1-$\alpha7$, and lynx2-$\alpha7$) are not significantly different ($p = 0.16$). Therefore, we concluded that lynx2-$\alpha3\beta4$ interaction is significantly stronger than the other three interactions, reflected by the fitted lines' similar slope and significantly higher intercept than the other interactions. This supports that
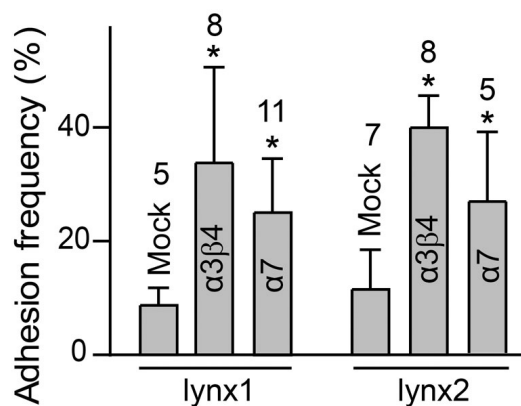

FIGURE 2 The binding frequency between lynx1 or lynx2 and mock, $\alpha3\beta4$-nicotinic acetylcholine receptor (nAChR)-expressing or $\alpha7$-nAChR expressing cells. The control experiment was conducted between lynx1 or lynx2 and WT (mock) cells that did not express nAChRs. Thirty percentage binding frequency indicates the detection of single molecular interactions. The total tested cell numbers (N) for each group are labeled above each bar. The raw data to generate the plot are summarized in Table S1. The error bar represents the standard deviation of the binding frequencies of the multiple cells in each group. Asterisks indicate $p < 0.05$ compared to control groups by unpaired T-test
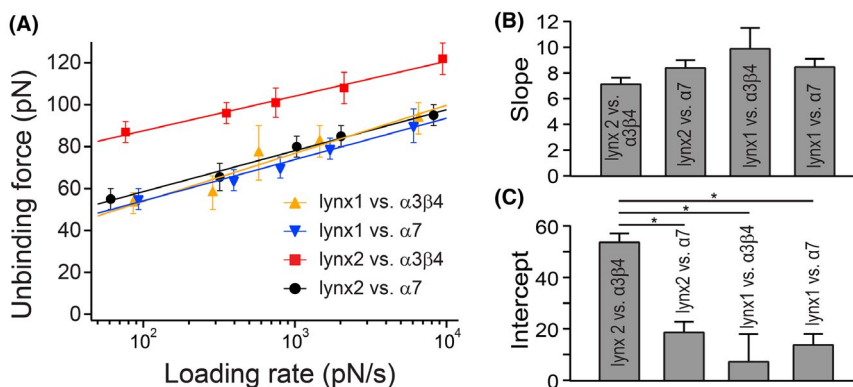
FIGURE 3 (A) The dynamic force spectra (i.e., the plot of most probable unbinding force (F_u^*)) as a function of loading rate (r_f) of the lynx-nicotinic acetylcholine receptor (nAChR) interactions in Equation (3). The most probable unbinding forces of the lynx1-nAChR (orange, blue) and lynx2-nAChR (red, black) interactions were obtained from the center of the tallest bin of each unbinding force histograms (Figure S2). The data are fitted by linear regression to the single-barrier Bell–Evans model (solid lines, Equation 3) to extract the off-rate k^0.[49] The bars denote half bin widths of the unbinding force histograms (shown in Figure S2), representing the force determination error. (B) Comparison of the fitted slopes of the linear regression. Statistical analysis of the linear regression was conducted using Analysis of Covariance (ANCOVA), which indicated the difference of the slopes of the four linear regression fits is insignificant ($p = 0.24$). (C) Comparison of the fitted intercepts of the linear regression. *Significant difference ($p < 0.001$) revealed by the ANCOVA analysis

TABLE 1 Summary of Bell–Evans fit results for lynx-nicotinic acetylcholine receptor binding

	lynx1		lynx2	
Parameters	α3β4	α7	α3β4	α7
k^0: (s^{-1})	0.045 ± 0.036	0.021 ± 0.011	$7.4 \times 10^{-5} \pm 6.3 \times 10^{-5}$	0.012 ± 0.006
γ: (nm)	0.41 ± 0.06	0.48 ± 0.03	0.57 ± 0.04	0.48 ± 0.03

k^0 is the unstressed off-rate of the interaction. γ the energetic barrier distance between the bound state and transition state along the reaction coordinate. The errors are the stand error of the fits.
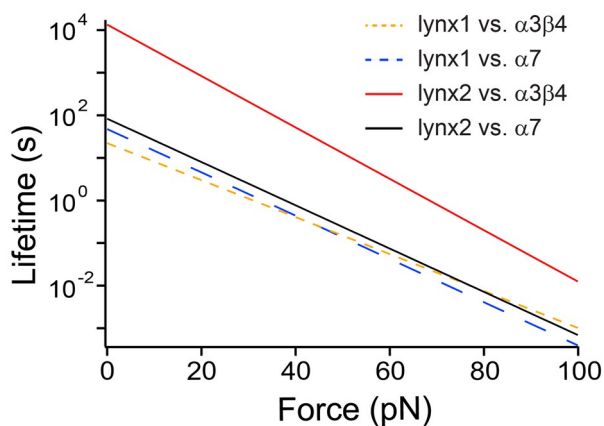

FIGURE 4 Comparison of lifetimes of the lynx-nicotinic acetylcholine receptor complexes as a function of force. Lifetimes are giving by Equation (1) using the parameters taken from Table 1

The Bell–Evans model also allows the estimation of lynx-receptor association lifetime at different constant pulling forces (Equation 1). Taking the off-rates and barrier position parameters from Table 1, we compared the lifetime of lynx-receptor associations as a function of force (Figure 4). At no force, the lifetime of a lynx2-α3β4 interaction was estimated to be 10^4 s and was more than two orders of magnitude longer than the lifetimes of the lynx1-α3β4, lynx1-α7, and lynx2-α7 interactions. The lifetimes of all interactions decreased exponentially as a function of pulling force. However, a ~100-fold difference was observed between lynx2-α3β4 and the other three pairs at different pulling forces. This indicates that compared to the other three interaction pairs, α3β4 and lynx2 can remain bound for a much more extended period and that lynx2 may play a much more significant role in regulating the activity of α3β4-nAChR−expressing neurons.

the α3β4-nAChR bound to lynx1 and lynx2 differentially and may be due to different lynx1-α3β4 and lynx2-α3β4 binding interfaces. Table 1 also indicates that lynx1 binds α7 with a comparable affinity of α3β4, while lynx2 strongly preferred binding to α3β4.

4 | DISCUSSION

The current study demonstrates the utility of AFM as a quantitative means for capturing the relative differences in lynx affinity for nAChR subtypes. Prior studies have been

carried out using a range of assays, including in vitro,[22,23] ex vivo slice,[9] single-unit and VEP whole animal[20,50] recordings, as well as co-immunoprecipitation pull-downs,[24,51] bungarotoxin competition[32] and fluorescent flux measurements.[27] These varied approaches complicate elucidation of the relative effects of different lynx proteins on their cognate receptor subtypes. The pan-specific nature of lynx binding on multiple nAChR subtypes warrants a more systematic approach to quantitatively measure specific binding in a nonneuronal system that expresses a singular nAChR subtype, unlike neurons, which can express multiple subtypes. A further complication is that lynx1 has been shown to alter receptor number when co-expressed in the same cell with nAChR subtypes.[23,27] By avoiding such co-expression, single-molecule studies by AFM can eliminate potential apparent functional changes (e.g., E_{max}) that might come as a consequence of changes in receptor number.

Previous binding studies have been carried out using radiolabeled α-bungarotoxin competition in cells[32] or in brain homogenates.[51] The α-bungarotoxin competition studies have produced K_d values, but α-bungarotoxin preferentially binds to α7 and muscle nAChR subtypes and is less useful for the study of other nAChR subtypes. AFM offers a method of comparing and quantitating binding across multiple nAChR subtypes in a cellular and membrane environment reminiscent of the neuronal one.

Lynx1 and lynx2 have complex allosteric biophysical functions on nAChRs, as they are shown to alter nAChR EC_{50},[22] E_{max},[23,27] IC_{50},[32] desensitization kinetics[22,24] and stoichiometry.[52] Quantifying the unbinding force between lynx and nAChRs isolates the effect of protein-receptor affinity from the other functional effects on the receptor. Because lynx has been shown to influence the aforementioned characteristics, limiting studies to one effect has significant implications for understanding lynx's biophysical mechanism of action. If two lynx2 mutants have similar binding affinities to the same α3β4-nAChR in AFM experiments but influence receptor activity differentially in functional studies, a case may be made that the mutants alter neuron function via agonist affinity, desensitization kinetics, etc.

Our studies use a water-soluble version of lynx proteins, although native lynx is a GPI-anchored protein. Studies using water-soluble lynx1 have demonstrated its structural homology with α-neurotoxins by NMR and its similar modulatory effects to native lynx,[26,53] making it a viable model for functional and binding studies. Nevertheless, the unbinding force of the lynx-nAChR interaction may differ between the soluble and native lynx proteins since some differential functional effects have been reported depending on the presence of the GPI anchor on lynx1.[16,18,22,23,54] The GPI anchor can also impose constraints because it has an affinity for cholesterol-rich domains,[18,55,56] which may influence local concentrations of nAChR and lynx proteins and their lateral mobility.

The studies on receptor lifetime are interesting considering our recent molecular dynamics studies on the interactions of GPI-anchored lynx1 and α4β2-nAChRs.[57] Molecular dynamics simulations indicate relatively stable interactions between lynx1 and the C-loop of the α4:α4 interface of the nAChR, an important subregion for nAChR state transitions, as well as on the complementary face of the subunit adjacent to the C-loop. Interestingly, the interactions observed between lynx1 and the nAChR show some nondeterministic influences on the C-loop behavior, such as preventing a closed C-loop from reopening (keeping the intermediate state between open and closed) or maintaining the C-loop open state, depending on lynx1's location relative to the C-loop. Therefore, it will be interesting to model and simulate lynx2 and α3β4-nAChR for possible prolonged interactions at such critical sites for nAChR function.

This study demonstrates the reliability of AFM to capture binding energies between immobilized lynx proteins and nAChR subtypes expressed on SH-EP cells. The physiological and pathological implications of these lynx-nAChR affinities remain to be fully elucidated via in vivo experiments, however. The stronger affinity of lynx2 for α3β4- over α7-nAChRs, if borne out in vivo, might be associated with nicotine aversion. α3β4-nAChRs are highly expressed in the MHbV-IPN pathway and have been implicated in restricting high- dose nicotine intake.[58] The degree to which lynx protoxins can extend nAChR closed times[23] or inhibit recovery from desensitization[22] could result in significant effects on activity in this region and thus be a factor in nicotine intake.

Lynx-nAChR subtype combinations not explored in our experiment should also be tested under both AFM and functional studies. This can be helpful for understanding not only nicotine-dependence via the study of interactions between lynx1 and α5- or α4β2-nAChRs, for example, but also many other nAChR-dependent processes. One could more deeply investigate the modulatory effects of lynx on α4β2-nAChRs as they relate to anxiety and visual plasticity,[20,24] the lynx1−α7-nAChR and lynx1−β2-containing nAChR interactions that pertain to neuronal health[9] and other lynx-nAChR combinations relevant in Alzheimer's disease.[51]

Lynx mutants can also be tested against nAChRs to determine which lynx residues influence lynx-nAChR binding significantly. Structure-function AFM studies can test naturally occurring mutations or residues selected through molecular modeling or neutral scans. Studies on concatemeric receptors with fixed stoichiometries can be used to address outstanding questions about the preference of lynx for specific stoichiometries or specific nAChR subunit interfaces. Previous studies indicate preferential

binding of lynx1 at the α:α interfaces of the nAChRs with either $(\alpha3\beta4)_2\alpha3$ or $(\alpha4)_3(\beta2)_2$ stoichiometry[23,52] but have not excluded less-preferred binding at other interfaces. Such questions are suitable for an approach such as AFM, which can quantitate the strength of binding. Multiple members of lynx proteins exist in the brain and body. Testing these on a range of nAChR subtypes via AFM can reveal novel interactions, leading to new investigations of biological importance and a targeted understanding of how specific interactions in a widespread neurotransmitter system underlie various neurological states.

CONFLICT OF INTEREST
All authors declare that they have no conflict of interest in connection with this article.

AUTHOR CONTRIBUTIONS
Julie M. Miwa and X. Frank Zhang designed research; Paul Whiteaker contributed reagents; Avani V. Pisapati and Wenpeng Cao performed research; Wenpeng Cao, Griffin Jones, Kristin Anderson, and Katie Holick Hoffman performed biochemistry research; Avani V. Pisapati, Wenpeng Cao, and X. Frank Zhang analyzed data; Avani V. Pisapati, Wenpeng Cao, Kristin R. Anderson, Katie Hoffman Holick, Paul Whiteaker, Wonpil Im, Julie M. Miwa, and X. Frank Zhang wrote the paper.

ORCID
X. Frank Zhang https://orcid.org/0000-0002-8778-595X

REFERENCES
1. Xu X, Bishop EE, Kennedy SM, Simpson SA, Pechacek TF. Annual healthcare spending attributable to cigarette smoking: an update. *Am J Prev Med*. 2015;48:326-333.
2. In the health consequences of smoking-50 years of progress: a report of the surgeon general. Atlanta, GA, 2014.
3. Nicholatos JW, Francisco AB, Bender CA, et al. Nicotine promotes neuron survival and partially protects from Parkinson's disease by suppressing SIRT6. *Acta Neuropathol Commun*. 2018;6:120.
4. Lucatch AM, Lowe DJE, Clark RC, Kozak K, George TP. Neurobiological determinants of tobacco smoking in Schizophrenia. *Front Psychiatry*. 2018;9:672.
5. Gotti C, Clementi F, Fornari A, et al. Structural and functional diversity of native brain neuronal nicotinic receptors. *Biochem Pharmacol*. 2009;78:703-711.
6. Wu J, Lukas RJ. Naturally-expressed nicotinic acetylcholine receptor subtypes. *Biochem Pharmacol*. 2011;82:800-807.
7. Hurst R, Rollema H, Bertrand D. Nicotinic acetylcholine receptors: from basic science to therapeutics. *Pharmacol Ther*. 2013;137:22-54.
8. Araud T, Graw S, Berger R, et al. The chimeric gene CHRFAM7A, a partial duplication of the CHRNA7 gene, is a dominant negative regulator of alpha7*nAChR function. *Biochem Pharmacol*. 2011;82:904-914.
9. Miwa JM, Stevens TR, King SL, et al. The prototoxin lynx1 acts on nicotinic acetylcholine receptors to balance neuronal activity and survival in vivo. *Neuron*. 2006;51:587-600.
10. Steinlein OK, Hoda J-C, Bertrand S, Bertrand D. Mutations in familial nocturnal frontal lobe epilepsy might be associated with distinct neurological phenotypes. *Seizure*. 2012;21:118-123.
11. Bertrand D. Neuronal nicotinic acetylcholine receptors and epilepsy. *Epilepsy Currents*. 2002;2:191-193.
12. Weltzin MM, Lindstrom JM, Lukas RJ, Whiteaker P. Distinctive effects of nicotinic receptor intracellular-loop mutations associated with nocturnal frontal lobe epilepsy. *Neuropharmacology*. 2016;102:158-173.
13. Lee HW, Yang SH, Kim JY, Kim H. The role of the medial habenula cholinergic system in addiction and emotion-associated behaviors. *Front Psychiatry*. 2019;10:100.
14. Fowler CD, Kenny PJ. Habenular signaling in nicotine reinforcement. *Neuropsychopharmacology*. 2012;37:306-307.
15. Antolin-Fontes B, Ables JL, Gorlich A, Ibanez-Tallon I. The habenulo-interpeduncular pathway in nicotine aversion and withdrawal. *Neuropharmacology*. 2015;96:213-222.
16. Miwa JM, Ibañez-Tallon I, Crabtree GW, et al. lynx1, an endogenous toxin-like modulator of nicotinic acetylcholine receptors in the mammalian CNS. *Neuron*. 1999;23:105-114.
17. Galat A, Gross G, Drevet P, Sato A, Menez A. Conserved structural determinants in three-fingered protein domains. *FEBS J*. 2008;275:3207-3225.
18. Miwa JM, Anderson KR, Hoffman KM. Lynx prototoxins: roles of endogenous mammalian neurotoxin-like proteins in modulating nicotinic acetylcholine receptor function to influence complex biological processes. *Front Pharmacol*. 2019;10:343.
19. Miwa JM, Freedman R, Lester HA. Neural systems governed by nicotinic acetylcholine receptors: emerging hypotheses. *Neuron*. 2011;70:20-33.
20. Morishita H, Miwa JM, Heintz N, Hensch TK. Lynx1, a cholinergic brake, limits plasticity in adult visual cortex. *Science*. 2010;330:1238-1240.
21. Shenkarev ZO, Shulepko MA, Bychkov ML, et al. Water-soluble variant of human Lynx1 positively modulates synaptic plasticity and ameliorates cognitive impairment associated with alpha7-nAChR dysfunction. *J Neurochem*. 2020;155:45-61.
22. Ibanez-Tallon I, Miwa JM, Wang HL, et al. Novel modulation of neuronal nicotinic acetylcholine receptors by association with the endogenous prototoxin lynx1. *Neuron*. 2002;33:893-903.
23. George AA, Bloy A, Miwa JM, Lindstrom JM, Lukas RJ, Whiteaker P. Isoform-specific mechanisms of alpha3beta4*-nicotinic acetylcholine receptor modulation by the prototoxin lynx1. *FASEB J*. 2017;31:1398-1420.
24. Tekinay AB, Nong Y, Miwa JM, et al. A role for LYNX2 in anxiety-related behavior. *Proc Natl Acad Sci U S A*. 2009;106:4477-4482.
25. Dessaud E, Salaun D, Gayet O, Chabbert M, deLapeyriere O. Identification of lynx2, a novel member of the ly-6/neurotoxin superfamily, expressed in neuronal subpopulations during mouse development. *Mol Cell Neurosci*. 2006;31:232-242.
26. Lyukmanova EN, Shenkarev ZO, Shulepko MA, et al. NMR structure and action on nicotinic acetylcholine receptors of water-soluble domain of human LYNX1. *J Biol Chem*. 2011;286:10618-10627.
27. Wu M, Puddifoot CA, Taylor P, Joiner WJ. Mechanisms of inhibition and potentiation of alpha4beta2 nicotinic acetylcholine

receptors by members of the Ly6 protein family. *J Biol Chem.* 2015;290:24509-24518.

28. Breining SR, Melvin M, Bhatti BS, et al. Structure-activity studies of 7-heteroaryl-3-azabicyclo[3.3.1]non-6-enes: a novel class of highly potent nicotinic receptor ligands. *J Med Chem.* 2012;55:9929-9945.

29. Zhang X, Rico F, Xu AJ, Moy V. Atomic force microscopy of protein-protein interactions. In: Hinterdorfer P, van Oijen A eds. *Handbook of Single-Molecule Biophysics.* Springer Press; 2009:555-570. https://link.springer.com/chapter/10.1007/978-0-387-76497-9_19

30. Zhang XH, Chen A, Wojcikiewicz E, Moy VT. Probing ligand-receptor interactions with atomic force microscopy. In: Golemis EA, ed. *Protein-Protein Interactions: A Molecular Cloning Manual.* Woodbury, NY: Cold Spring Harbor Laboratory Press; 2002:241-254.

31. Binnig G, Quate CF, Gerber C. Atomic force microscope. *Phys Rev Lett.* 1986;56:930-933.

32. Kryukova EV, Egorova NS, Kudryavtsev DS, et al. From synthetic fragments of endogenous three-finger proteins to potential drugs. *Front Pharmacol.* 2019;10:748.

33. Zhao L, Kuo YP, George AA, et al. Functional properties of homomeric, human alpha 7-nicotinic acetylcholine receptors heterologously expressed in the SH-EP1 human epithelial cell line. *J Pharmacol Exp Ther.* 2003;305:1132-1141.

34. Lukas RJ, Fryer JD, Eaton JB, Gentry CL. Some methods for studies of nicotinic acetylcholine receptor pharmacology. In *Nicotinic Receptors in the Nervous System.* CRC Press; 2001:3-28.

35. Zhang XH, Wojcikiewicz E, Abdulreda M, Chen A, Moy VT. Probing ligand-receptor interactions with atomic force microscopy. In Golemis EA, Adams PD eds. *Protein-Protein Interactions: A Molecular Cloning Manual.* 2nd ed. ; 2005:399-413.

36. Ebner A, Wildling L, Kamruzzahan AS, et al. A new, simple method for linking of antibodies to atomic force microscopy tips. *Bioconjug Chem.* 2007;18:1176-1184.

37. Wildling L, Unterauer B, Zhu R, et al. Linking of sensor molecules with amino groups to amino-functionalized AFM tips. *Bioconjug Chem.* 2011;22:1239-1248.

38. Hutter JL, Bechhoefer J. Calibration of atomic-force microscope tips. *Rev Sci Instrum.* 1993;64:1868-1873.

39. Dragovich MA, Fortoul N, Jagota A, et al. Biomechanical characterization of TIM protein-mediated Ebola virus-host cell adhesion. *Sci Rep.* 2019;9:267.

40. Zhang S, Hu LA, Du HG, et al. BF0801, a novel adenine derivative, inhibits platelet activation via phosphodiesterase inhibition and P2Y(12) antagonism. *Thromb Haemost.* 2010;104:845-857.

41. Du D, Xu FL, Yu LH, et al. The tight junction protein, occludin, regulates the directional migration of epithelial cells. *Dev Cell.* 2010;18:52-63.

42. Zhang XH, Chen A, De Leon D, et al. Atomic force microscopy measurement of leukocyte-endothelial interaction. *American Journal of Physiology-Heart and Circulatory Physiology.* 2004;286:H359-H367.

43. Franz CM, Taubenberger A, Puech PH, Muller DJ. Studying integrin-mediated cell adhesion at the single-molecule level using AFM force spectroscopy. *Science's STKE* 2007:pl5.

44. Helenius J, Heisenberg CP, Gaub HE, Muller DJ. Single-cell force spectroscopy. *J Cell Sci.* 2008;121:1785-1791.

45. Hinterdorfer P, Dufrene YF. Detection and localization of single molecular recognition events using atomic force microscopy. *Nat Methods.* 2006;3:347-355.

46. Rico F, Zhang XH, Moy VT. Probing cellular adhesion at the single molecular level. In: Life at the Nanoscale – Atomic Force Microscopy of Live Cells. Pan Stanford Publishing; 2011:225-262.

47. Bell GI. Models for the specific adhesion of cells to cells. *Science.* 1978;200:618-627.

48. Evans E, Ritchie K. Dynamic strength of molecular adhesion bonds. *Biophys J.* 1997;72:1541-1555.

49. Chesla SE, Selvaraj P, Zhu C. Measuring two-dimensional receptor-ligand binding kinetics by micropipette. *Biophys J.* 1998;75:1553-1572.

50. Fan LZ, Kheifets S, Bohm UL, et al. All-optical electrophysiology reveals the role of lateral inhibition in sensory processing in cortical layer 1. *Cell.* 2020;180(521–535):e518.

51. Thomsen MS, Andreasen JT, Arvaniti M, Kohlmeier KA. Nicotinic acetylcholine receptors in the pathophysiology of Alzheimer's disease: the role of protein-protein interactions in current and future treatment. *Curr Pharm Des.* 2016;22:2015-2034.

52. Nichols WA, Henderson BJ, Yu C, et al. Lynx1 shifts alpha-4beta2 nicotinic receptor subunit stoichiometry by affecting assembly in the endoplasmic reticulum. *J Biol Chem.* 2014;289:31423-31432.

53. Lyukmanova EN, Shulepko MA, Buldakova SL, et al. Water-soluble LYNX1 residues important for interaction with muscle-type and/or neuronal nicotinic receptors. *J Biol Chem.* 2013;288:15888-15899.

54. Miwa JM, Walz A. Enhancement in motor learning through genetic manipulation of the Lynx1 gene. *PLoS One.* 2012;7:e43302.

55. Lester HA, Miwa JM, Srinivasan R. Psychiatric drugs bind to classical targets within early exocytotic pathways: therapeutic effects. *Biol Psychiatry.* 2012;72:907-915.

56. Li J, Liu X, Tian F, Yue T, Zhang X, Cao D. Spontaneous insertion of GPI anchors into cholesterol-rich membrane domains. *AIP Adv.* 2018;8:055210. http://dx.doi.org/10.1063/1.5024036

57. Dong C, Kern NR, Anderson KR, Zhang XF, Miwa JM, Im W. Dynamics and interactions of GPI-linked lynx1 protein with/without nicotinic acetylcholine receptor in membrane bilayers. *J Phys Chem B.* 2020;124:4017-4025.

58. Frahm S, Ślimak MA, Ferrarese L, et al. Aversion to nicotine is regulated by the balanced activity of β4 and α5 nicotinic receptor subunits in the medial habenula. *Neuron.* 2011;70:522-535. http://dx.doi.org/10.1016/j.neuron.2011.04.013

SUPPORTING INFORMATION

Additional supporting information may be found in the online version of the article at the publisher's website.